Inorganic Chemistry Communications 124 (2021) 108409

Contents lists available at ScienceDirect

Inorganic Chemistry Communications

journal homepage: www.elsevier.com/locate/inoche

Quantum chemical and molecular dynamic simulation studies for the identification of the extracted cinnamon essential oil constituent responsible for copper corrosion inhibition in acidified 3.0 wt% NaCl medium

K. Dahmani [a], M. Galai [b], M. Ouakki [a], M. Cherkaoui [a,c], R. Touir [b,d,*], S. Erkan [e], S. Kaya [f], B. El Ibrahimi [g]

[a] Organic Chemistry, Catalysis and Environment Laboratory, Faculty of Science, Ibn Tofail University, Kenitra, Morocco
[b] Advanced Materials and Process Engineering Laboratory, Faculty of Science, Ibn Tofail University, Kenitra, Morocco
[c] National Higher School of Chemistry (NHSC), University Ibn Tofail BP. 133-14000, Kenitra, Morocco
[d] Regional Center for Education and Training Professions (CRMEF), Kenitra, Morocco
[e] Chemistry and Chemical Processing Technologies, Sivas Cumhuriyet University, Yıldızeli Vocational School Sivas, Turkey
[f] Sivas Cumhuriyet University, Health Services Vocational School, Department of Pharmacy, 58140 Sivas, Turkey
[g] Team of Physical Chemistry and Environment, Faculty of Science, Ibn Zohr University, Agadir, Morocco

ARTICLE INFO

Keywords:
Green inhibitor
Copper
Acidified 3.0 wt% NaCl solution
Electrochemical measurements
Surface analysis
Theoretical study

ABSTRACT

The influence of the extracted cinnamon essential oil (CiO) on the copper corrosion resistance in acidified 3.0 wt % NaCl (pH = 2) medium was investigated by using electrochemical measurements and Scanning Electron Microscopy (SEM) with Energy Dispersive X-Ray Analysis (EDS). So, in order to identify the component of CiO responsible for corrosion inhibition of copper in corrosive solution, the density functional theory (DFT) calculations and molecular dynamics simulation were used. Potentiodynamic polarization showed that the tested natural product acts as cathodic-type inhibitor. Electrochemical impedance spectroscopy indicated that the inhibition efficiency increases with CiO concentrations to get up a maximum value of 89% at 200 ppm. In addition, SEM/EDS analysis in the presence of 200 ppm CiO indicated that copper surface was exempt for all corrosion products, confirming its offered protection. Finally, the major calculated quantum chemical descriptors obtained from DFT calculations indicated that the anticorrosion efficiency responsibility attributes to P8 and P46, with the predominance of P8. In the same, the molecular dynamics simulation indicated that the adsorption energy follows the order: P5 (-61.071 kJ mol^{-1}) > P46 (-58.070 kJ mol^{-1}) > P8 (-42.938 kJ mol^{-1}) on Cu (1 1 1) and P8 (-21.220 kJ mol^{-1}) > P46 (-20.066 kJ mol^{-1}) > P5 (-19.591 kJ mol^{-1}) on CuO_2 (1 1 0), suggesting a strong adsorption of P8 on oxide copper (1 1 0) surface and consequently therefore the performance of extracted CiO can be attributed to P8, which is parallel to the copper (1 1 1) surface contrary to other molecules P46 and P5.

1. Introduction

Metallic copper is widely used in many industrial applications because of its respectable properties such as electrical, thermal and mechanical proprieties [1]. So, its corrosion remains an important problem, especially in environments containing chloride ions [2–9]. On the other hand, it is known that the chloride ions influence the anodic reaction of copper, which its presence done the formation of CuCl layer. So, this layer partially protects the copper surface and it is transformed to the soluble species ($CuCl_2^-$) [10].

Therefore, protection of copper surface against corrosion has become a major problem in a corrosive environment. Its inhibition using several types of heterocyclic compounds has been reported [11–16]. These compounds can form an adsorbed protective layer on the copper surface via polar functional groups such as -N, -S, -O and/or conjugated double bonds and block the active surface sites.

With the increasing environmental awareness, the exploitation of environmental friendly compounds is one of the focus researches

* Corresponding author.
E-mail addresses: touir8@yahoo.fr, touir8@gmail.com (R. Touir).

https://doi.org/10.1016/j.inoche.2020.108409
Received 30 October 2020; Received in revised form 9 December 2020; Accepted 13 December 2020
Available online 29 December 2020

Table 1
Chemical composition of Cinnamon essential oil extraction.

Retention time (min)	Compounds names	Indicative values (wt. %)
3.01	α-phellandrene	0.01
3.06	D 3-Carene	0.02
3.10	α -terpinene	0.01
3.16	p-cymene	0.21
3.20	Limonene	0.17
3.23	1,8-cineole	0.13
3.29	Phenylacetaldehyde	0.02
3.42	γ-terpinene	0.05
3.47	acetophenone	0.09
3.65	Terpinolene	0.07
3.71	trans β-ocimene	0.04
3.80	α -Thujone	0.11
3.88	β -Thujone	0.23
4.00	Benzene terbutyl	0.28
4.10	2-methyl benzofuran	0.02
4.12	Camphor	0.28
4.23	hydrocinnamaldehyde	1.64
4.28	Borneol	0.42
4.36	Terpinen-4-ol	0.07
4.46	α -terpinol	0.20
4.50	Estragole	Trace
4.69	Cis cinnamaldehyde	1.62
4.86	Cuminicaldehyde	1.27
5.28	**Transcinnamaldehyde**	**46.30**
5.72	Eugenole	0.12
5.82	α - copaene	1.36
5.89	**β - Cubebene**	**5.20**
5.96	β -selinene	0.43
5.98	Valancene	0.38
6.02	Viridiflorene	0.62
6.23	α -Logipinene	0.29
6.52	α -murolene	3.97
6.68	γ -cadinene	4.84
6.83	**δ-cadinene**	**8.16**
7.48	Cubenol	1.69
7.57	T-Cadinol	4.58
7.75	Cadalene	1.21
8.22	Benzyl benzoate	0.10

[17–20]. In the same context, some studies have focused on the environmental, efficient, cheap and sustainable use of the compounds in many industrial applications [21–23].

Currently, investigation in copper corrosion in several media is oriented to the development of eco-friendly and biodegradability inhibitors; compounds with good inhibitory efficiency, but low or zero risk of environmental pollution [24–27]. However, to continue our research on the investigation of the eco-friendly compounds, the effect of CiO on the copper and coating corrosion in sulfuric acid medium have reported [28,29]. It is shown that the corrosion resistance of copper in sulfuric acid and its coating developed on interconnections have remarkably improved with the CiO addition.

On the other hand, it is well-known that theoretical study is one of the most important methods used for the elucidation for the interaction inhibitor molecules/surface metal. Many researches were employed for the study of anticorrosion copper in chloride solutions [30–32].

In order to continue our research on the investigation of green compounds, the effect of extracted CiO on copper corrosion in acidified 3.0 wt% NaCl medium was studied by using electrochemical measurements and surface characterization. Then, both DFT calculations and MD simulations were adopted to determine the responsible of corrosion inhibition of the major constituents of extracted CiO on copper surface, which has not been reported previously according to our knowledge.

2. Experimental and theoretical studies

2.1. Green inhibitor

The plant of cinnamon (where its name is referred to its mid-brown color) is a spice obtained from the inner bark of some Cinnamomum trees, which is used in sweet and savory foods. In addition, cinnamon is also the name of a dozen species of trees and commercial spice products, which are of the species Cinnamomum in the Lauraceae family. One a few of them are grown commercially for spices [28]. This plant was identified and their most contents were extracted by hydro-distillation in a Clevenger-type apparatus at 100 °C for five hours. The obtained oil was isolated and kept in a dark glass in the refrigerator until required for further use. It was analyzed by gas chromatography coupled to mass spectrometry (GC–MS) using the Thermo Fisher apparatus. Thus, 38 compounds were found as presented in Table 1, where the major constituents are mainly *trans*-cinnamaldehyde (46.30 wt%) (noted: P46), δ-cadinene (8.16 wt%) (Noted: P8) and β-cubebene (5.20 wt%) (Noted: P5), where their molecular structures are presented in Fig. 1 [28].

2.2. Corrosive medium and copper specimens

The chemical products of NaCl and sulfuric acid were purchased from Sigma-Aldrich and used as received. So, the used corrosive medium is a solution of 3.0 wt% NaCl acidify at pH = 2 in order to minimize the corrosion pitting action. This solution was prepared by dissolution of 3 g of NaCl in 100 mL of distilled water. To adjust pH to 2, the sulfuric acid solution was added. It was thermostatically fixed at 298 K in air atmosphere without bubbling for all measurements. Thus, the used copper's spacemen had the chemical composition: ≈ 0.5% of C, 0.5% ≈ of Mn, ≈ 0.05% of S, and the remainder Cu. It was manufactured to form a right cylinder, the cross-section of which was a disk about 1 cm in diameter (surface area S = 1 cm^2). The lateral part of the copper rod was firstly protected by a cataphoretic paint, heat treated at 150 °C, and then molded into an epoxy resin.

2.3. Electrochemical measurements

A conventional electrolysis cell with three electrodes assembly with the working electrode of copper, the platinum and saturated calomel

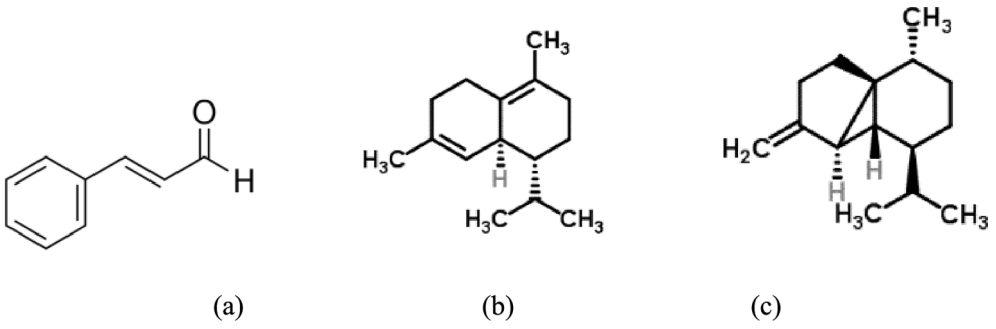

Fig. 1. Molecular structure of the major constituent of the extract cinnamon essential oils: (a) Trans-cinnamaldehyde (P46), (b) δ-cadinene (P8), and (c) β-Cubebene (P5).

(SCE) was used for electrochemical measurements by Potentiostat/Galvanostat PZC 100. Before each measurement, the substrate was polished with emery papers (from grade 600 to grade 1200), degreased with ethanol, washed with distilled water and finally dried in hot air.

The current–potential curves were recorded by changing the electrode potential automatically from negative (-1000 mV/SCE) to positive (+0.400 mV/SCE) values vs. E_{OCP} (Open circuit potential) with a scan rate of 0.2 mV/s after 1 h of immersion at 298 K. The kinetic corrosion parameters were extracted by using Stern Geary equation (1), using Origin software at the applied potential range of $E_{corr} \pm 0.100$ V/SCE:

$$i = i_a + i_c = i_{corr}\{exp[b_a \times (E - E_{corr})] - exp[b_c \times (E - E_{corr})]\} \quad (1)$$

where i_{corr} is the corrosion current density (A cm^{-2}), b_a and b_c are the Tafel constants of anodic and cathodic reactions (V^{-1}), respectively. The constants b_a and b_c are linked to the Tafel slopes β (V/dec) by equation (2):

$$\beta = \frac{ln10}{b} = \frac{2.303}{b} \quad (2)$$

Thus, the inhibition efficiency value was calculated as follows:

$$\eta_{PP} = \frac{i^0_{corr} - i_{corr}}{i^0_{corr}} \times 100 \quad (3)$$

where i^0_{corr} and i_{corr} are the corrosion current densities values in the absence and presence of CiO at different concentrations, respectively.

The electrochemical impedance measurements were made using the same equipment in the frequency interval from 100 kHz to 100 mHz with 5 points/decade (10 mV rms). The obtained diagrams were adjusted using EC-Lab program and the inhibition efficiency, η_{EIS}, was calculated as follows:

$$\eta_{EIS} = \frac{R_p - R^0_p}{R_p} \times 100 \quad (4)$$

Where R^0_p and R_p are the polarization resistance values without and with CiO at different concentrations, respectively.

All electrochemical experiments were performed between twice and three times. No significant discrepancy of the results was observed.

2.4. Scanning electron microscopy

The morphologies of the surface and the chemical composition of copper in acidified 3.0 wt% NaCl without and with the optimum concentration of extracted CiO after 16 h of immersion were determined by the scanning electron microscopy (SEM) instrument (SEM, JOEL JSM-5500) at 20 kV coupled with EDAX analysis.

2.5. DFT calculations

It is well-known that Conceptual Density Functional Theory (CDFT) [33] is one of the most important branches of Density Functional Theory. In the CDFT, chemical reactivity descriptors like chemical potential (μ), electronegativity (χ), hardness (η) and softness (σ) are described as the derivatives with respect to the number of electrons (N) of total electronic energy (E) at a constant external potential. While electronegativity is given as the negative value of chemical potential, softness is the multiplicative inverse of hardness. By applying finite differences approaches to the Conceptual Density Functional definitions of aforementioned chemical reactivity descriptors, the following equations including use of the ionization energy (I) and electron affinity (A) parameters have been obtained.

$$\chi = -\mu = -\left[\frac{\partial E}{\partial N}\right]_{\nu(r)} = \frac{I + A}{2} \quad (5)$$

$$\eta = \frac{1}{2}\left[\frac{\partial^2 E}{\partial N^2}\right]_{\nu(r)} = \frac{I - A}{2} \quad (6)$$

$$\sigma = 1/\eta \quad (7)$$

Within the framework of Koopmans Theorem [34], ionization energy and electron affinity values of molecules can be approximately predicted via HOMO and LUMO orbital energies, respectively. The theorem states that the negative values of HOMO and LUMO orbital energies correspond to ionization energy and electron affinity of molecules. If so, consider these information, one can write the relations $I = -E_{HOMO}$ and $A = -E_{LUMO}$. Electrophilicity index (ω) derived by Parr and al. correlates their electrophilic power with electronegativity (or chemical potential) and hardness of chemical species [35]. After this study, Chattaraj and al. defined the nucleophilicity (ε) as the multiplicative inverse of electrophilicity index [36].

In recent corrosion inhibition studies, two new parameters, namely electrodonating power and electroaccepting power, derived by Gazquez and al. are widely considered [37]. These parameters providing reliable information about electron donating and electron accepting abilities of molecules are formulated as follows:

$$\omega^+ = (I + 3A)^2/(16(I - A)) \quad (8)$$

$$\omega^- = (3I + A)^2/(16(I - A)) \quad (9)$$

The fraction of electrons transferred (ΔN) from inhibitor molecule to metal surface provides important clues about corrosion inhibition efficiencies. The equation proposed for the calculation of this parameter is based on chemical equalization principles. The equation for the calculation of ΔN values of adsorption processes is reported as:

$$\Delta N = \frac{\phi_{Cu} - \chi_{inh}}{2(\eta_{Cu} + \eta_{inh})} \quad (10)$$

wherein, it is important to note that χ_{inh}, η_{Cu} and η_{inh} stand for electronegativity of inhibitor, hardness of metal and hardness of inhibitor, respectively. In the calculations, $\eta_{Cu} = 0$ is taken, assuming that for a metallic bulk I = A. The work function value reported for Cu (1 1 1) surface is 4.80 eV [38].

2.6. Molecular Dynamic simulation approach

It is well-known that Molecular Dynamic Simulation approach [39] is an essential tool in the analysis of the nature of exchanges between inhibitor molecules and metal surfaces. The power of the interaction between inhibitor molecules and metal surface can be easily predicted via this approach [40,41]. Adsorption properties of studied molecules were investigated employing Forcite module from Accelrys Inc. The simulations were conducted in a box with the following dimensions 33 Å x 31 Å x 68 Å for Cu(1 1 1) and 34 Å x 30 Å x 74 Å CuO_2(1 1 0). The latest slabs were constructed from five layers of substrate and 60 Å as a vacuum region [42]. Calculations were repeated for both Cu (1 1 1) and Cu_2O (1 1 0) surfaces. Time of the simulation is 50 ps with 1 fs as step, while the temperature has been set to 298 K with the help of Anderson thermostat. To mimic the real situation, the aqueous phase has been considered in this work using 200 H_2O + $3Na^+$ + $3Cl^-$ solution formulation. Electrostatic interactions were estimated using Ewald summation method, whereas the Van der Waals interactions are computed via atom-based method [43,44]. In this part, interaction (or adsorption) and binding energy ($E_{binding}$) values of adsorption process were calculated as follows:

$$E_{adsorption} = E_{total} - (E_{surface+H_2O} + E_{inhibitor}) \quad (11)$$

$$E_{binding} = -E_{adsorption} \quad (12)$$

In the given equations, E_{total} stands for the total energy of all systems.

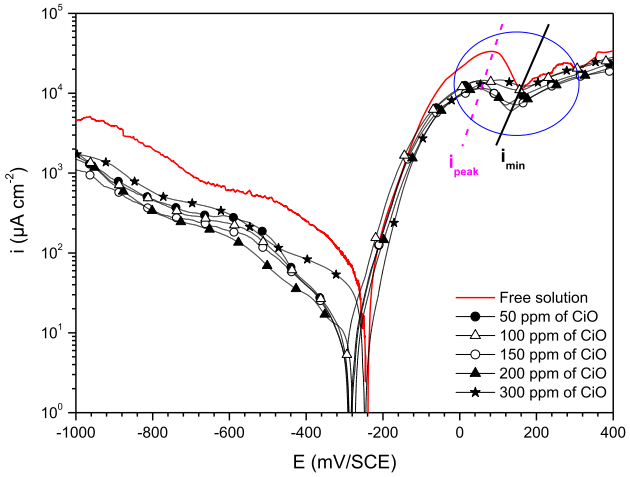

Fig. 2. Current – potential curves for copper in acidified 3.0 wt% NaCl without and with various concentrations of CiO after 1 h of immersion (sweep rate = 0.2 mV/s; T = 298 K).

$E_{surface+H2O}$ represents the total energy of substrate surface with solution. $E_{inhibitor}$ is the total energy of inhibitor alone. In the following section, the figures regarding to the adsorption process occurring between metal surfaces and studied inhibitor molecules give as detailed.

3. Results and discussion

3.1. Current – Potential measurements

The current–potential curves of copper in acidified 3.0 wt% NaCl solution at various concentrations of CiO are shown in Fig. 2 and their extracted corrosion parameters and inhibition efficiencies (η_{PP}) are illustrated in Table 2. However, i_{corr}, E_{corr}, β_a and β_c values are evaluated from the experimental results using the above equation (Equation (1)). In all cases, the correlation factor R^2 is greater than 0.99 indicating a good correlation between the experimental and fitting data (Fig. 3).

It can be noted that the current density values decrease with increasing of the concentrations of CiO, where the inhibition efficiency increases also to achieve a maximum value of 90.0% at 200 ppm (i.e. the corrosion current, i_{corr} , reduces from 35.6 μA cm^{-2} to 3.5 μA cm^{-2}). This result was probably due to the inhibitory effect of the three major constituents of CiO: P46, P8 and P5.

In addition, it's clear from Fig. 2 that, three different sections can be identified: first one, the Tafel region at lower over potentials extending to the peak current density (i_{peak}) (blue zone on Fig. 2). This phenomenon was attributed to the oxidation of copper into Cu^+ according to equation (13). The second region characterized by decreasing of current density until a minimum value which attributed to formation of CuCl according to equation (14). The last region characterized by a specific rapid increase in current density leading to a limiting value (i_{lim}), as a result of $CuCl_2^-$ formation according to equation (15), which is the responsible for the dissolution of Cu [45,46]. It has also been reported that the corrosion of Cu is initiated by oxygen and proceeds in two stages as follows [47]:

$$Cu \leftrightarrow Cu^+ + e^- \quad (13)$$

This Cu^+ ion reacts with chloride ions present in solution and forms CuCl,

$$Cu^+ + Cl^- \leftrightarrow CuCl \quad (14)$$

This has meagre hold, is incapable to defend the copper surface, and converts to the soluble cuprous chloride complex, $CuCl_2$,

$$CuCl + Cl^- \leftrightarrow CuCl_2^- \quad (15)$$

Under this condition, $CuCl_2^-$ is the principal species, forms at the surface of copper, and then diffuses into the majority solution. As there is no blocking film or layer of corrosion products, which they obtained by weight loss, quartz crystal microbalance, and scanning tunneling microscopy experiments [47].

However, the decreases in i_{corr}, i_{peak}, and i_{min} values are mainly explained by the reduction of chloride ion violence on the copper surface which attributed to the adhesion of CiO molecules. The negative move of the E_{corr} with the reduction in the oxygen content was appearing in the presence of CiO. This finding can be explained by the decrease in the rate of the cathodic reaction.

Moreover, the changes in the cathodic and anodic slopes of Tafel (β_c and β_a) are linked to the change of the cathodic and anodic reactions. This result indicates that the extracted CiO inhibit the corrosion process of copper by increasing its concentration as well as the oxygen content increases. This is in agreement with previous results where the role of oxygen and therefore the properties of the underlying Cu (I) oxide with aromatic heterocyclic compounds [48,49].

3.2. Impedance spectroscopy measurements

The Nyquist diagrams for copper in acidified 3.0% NaCl medium in the absence and presence of CiO at different concentrations after one

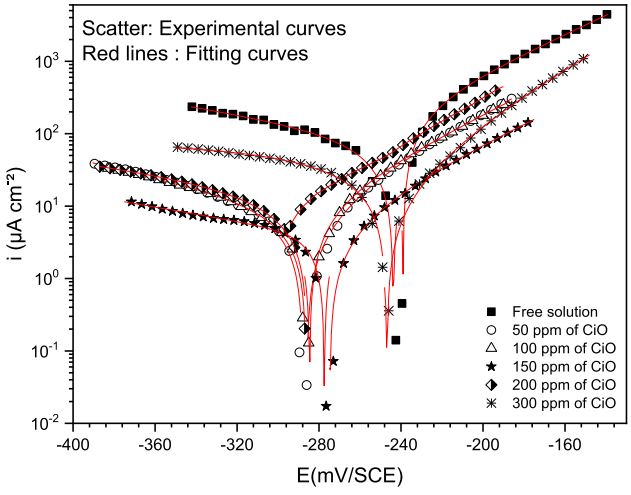

Fig. 3. Comparison of calculated and experimental data by mounting a non-linear fitting with equation (1).

Table 2
Electrochemical data and inhibition efficiency values of copper in acidified 3.0 wt% NaCl without and with different concentrations of extracted CiO (T = 298 K).

	C (ppm)	E_{corr} (mV/SCE)	i_{corr} (μA cm^{-2})	$-\beta_c$ (mV dec^{-1})	β_a (mV dec^{-1})	i_{peak} (mA cm^{-2})	i_{min} (mA cm^{-2})	η_{PP}(%)
Free solution	00	−239.0 ± 0.3	35.6 ± 2.1	145.1 ± 5.3	70.0 ± 3.3	32.46 ± 1.3	11.41 ± 1.2	–
Extracted CiO	50	−287.0 ± 0.4	4.5 ± 0.3	102.0 ± 4.1	50.0 ± 5.1	14.57 ± 2.1	11.02 ± 1.4	87.4
	100	− 287.0 ± 0.2	4.3 ± 0.2	111.2 ± 5.4	72.5 ± 3.7	13.59 ± 1.5	7.17 ± 1.1	88.0
	150	− 286.0 ± 0.1	4.0 ± 0.1	137.1 ± 3.8	53.0 ± 2.3	11.27 ± 1.2	7.50 ± 1.3	89.0
	200	−275.0 ± 0.2	3.5 ± 0.1	101.0 ± 4.2	62.0 ± 5.4	11.14 ± 1.3	6.07 ± 1.1	90.0
	300	−248.0 ± 0.3	5.6 ± 0.2	125.0 ± 3.3	69.4 ± 4.8	14.75 ± 2.1	12.23 ± 2.2	84.3

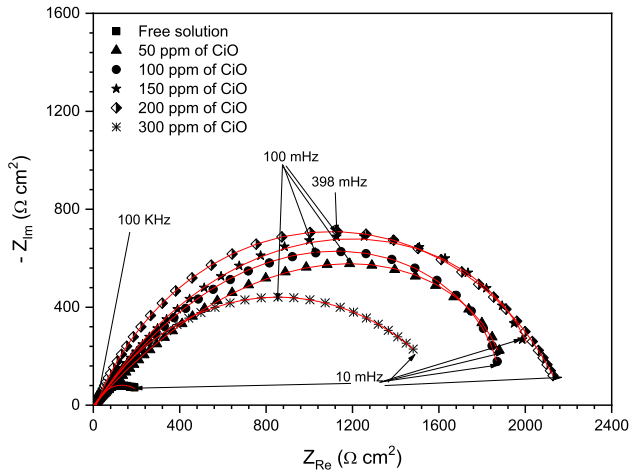

Fig. 4. Nyquist plots for copper in acidified 3.0 wt% NaCl solution without and with various concentrations of CiO at E_{OCP} (T = 298 K): Comparison of experimental (scatter) and fitting (red line) data. (For interpretation of the references to color in this figure legend, the reader is referred to the web version of this article.)

hour of immersion at E_{OCP} are presented in Fig. 4. Thus, the results obtained without CiO can be represented by a single capacitive loop, where those obtained by its presence were composed by two loops. Their extracted parameters using the equivalent circuit model (Fig. 5) are presented in Table 3. It can be noted that the increase of CiO concentration causes an increase of R_p value and a decrease of C_{dl} value from 467 μF cm^{-2} to 169 μF cm^{-2} at 200 ppm of CiO. This last finding may due to the reduction in the local dielectric constant and/or an increasing in the thickness of the electrical double layer, suggests that CiO operates by adsorption at the metal-solution interface [12]. On the other, the decrease in the C_{dl} value can be explained by the reducing of the access of charged species to the copper surface by the inhibitor molecules. In addition, the change in R_p and C_{dl} values was caused by the gradual replacement of H_2O molecules by the Cl^- anions present in the electrolyte and by the adsorption of the inhibitor molecules on the copper surface, which reduced its dissolution in this medium [13].

However, it is noted that the resistance value of the film (R_f) increases with inhibitor concentration, indicating that the extracted CiO stabilizes the corrosion products formed on the metal surface. This increase on R_f value was accompanied by a decreasing on the C_f values which can explained by that the elements of extracted CiO are adsorbed efficiently on the copper surface.

Finally, it is observed that the n_f and n_{dl} values increase with CiO concentrations signifying the rise of the copper surface homogeneity by

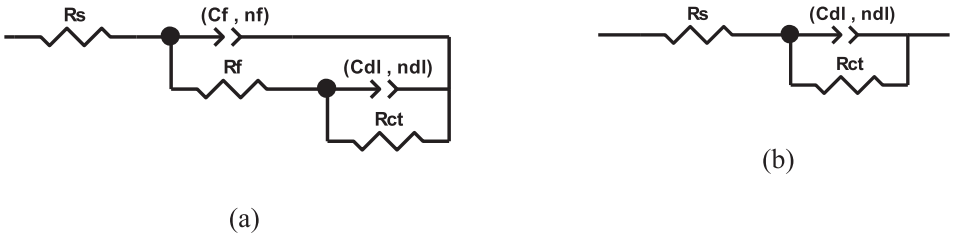

Fig. 5. Electrical equivalent circuit used to adjust the impedance spectra (a) in the presence of CiO (b) for free-solution.

Table 3
Electrochemical parameters for copper corrosion in acidified 3.0 wt% NaCl at various concentrations of extracted CiO at E_{OCP} (T = 298 K).

	C ppm	R_s Ω cm^2	C_f μF cm^{-2}	n_f	R_f Ω cm^{-2}	C_{dl} μF cm^{-2}	n_{dl}	R_{ct} Ω cm^2	R_p Ω cm^2	η_{EIS}%
Free solution	0	8.4 ± 1.1	–	–	–	467.0 ± 5.2	0.73 ± 0.01	249.0 ± 4.8	241	–
Extracted CiO	50	7.0 ± 1.0	102.0 ± 7.1	0.52 ± 0.01	488.0 ± 7.1	193.1 ± 3.4	0.74 ± 0.01	1455.0 ± 10.1	1943	87.6
	100	7.5 ± 0.7	98.1 ± 6.5	0.54 ± 0.01	509.0 ± 8.2	173.1 ± 5.7	0.75 ± 0.01	1507.0 ± 13.5	2016	88.0
	150	7.3 ± 0.8	42.0 ± 3.2	0.73 ± 0.01	641.0 ± 9.5	208.2 ± 6.4	0.82 ± 0.01	1498.0 ± 12.3	2139	88.7
	200	6.5 ± 0.5	24.2 ± 2.2	0.75 ± 0.01	650.0 ± 7.5	169.0 ± 5.1	0.84 ± 0.01	1547.0 ± 13.2	2197	89.0
	300	7.1 ± 1.1	155.0 ± 5.1	0.51 ± 0.01	320.0 ± 5.9	227.2 ± 5.3	0.81 ± 0.01	1305.0 ± 10.8	1625	85.2

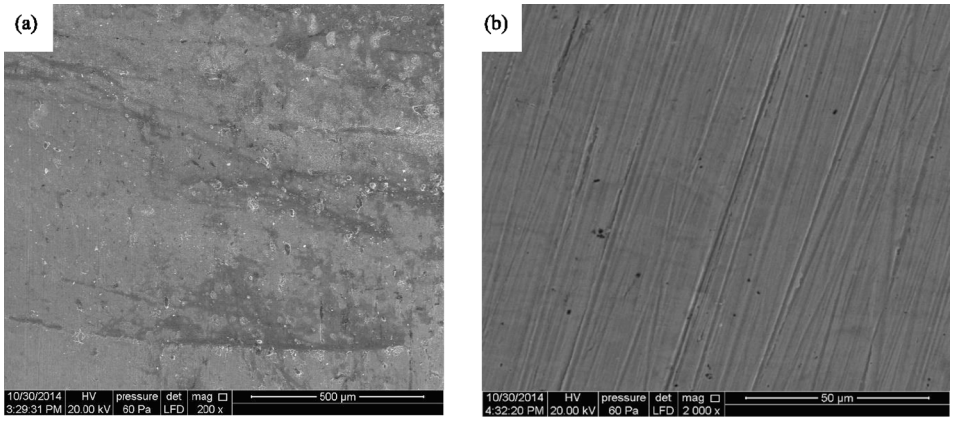

Fig. 6. SEM micrographs for copper surface in acidified 3.0 wt% NaCl after 16 h of immersion at E_{OCP} (T = 298 K) (a) without CiO, and (b) with 200 ppm CiO.

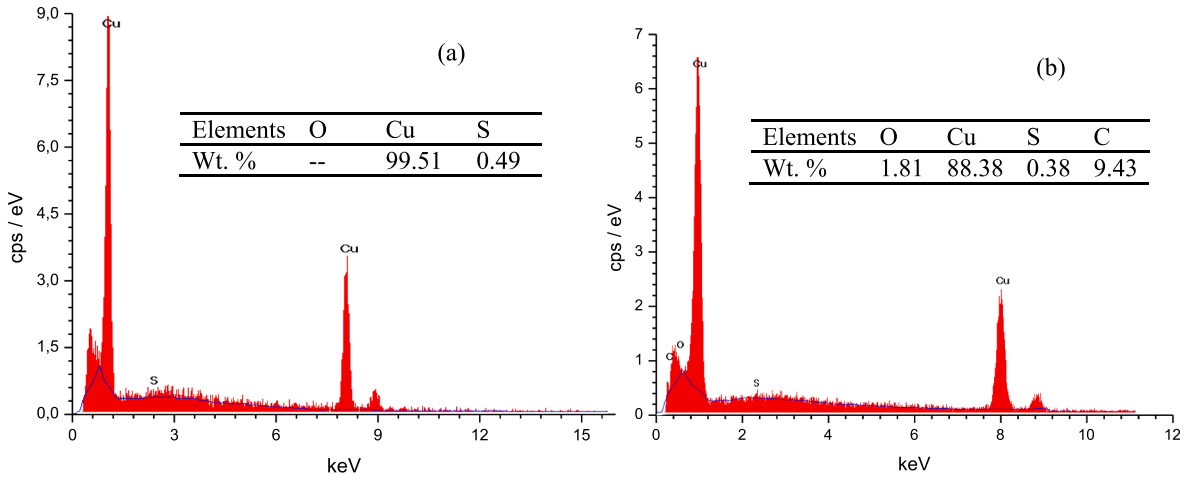

Fig. 7. EDS spectra for copper surface in acidified 3.0 wt% NaCl after 16 h of immersion at E_{OCP} (T = 298 K) (a) without CiO, and (b) with 200 ppm CiO.

reason of the inhibitor molecule adsorption on copper surface.

3.3. Scanning electron microscopy (SEM) and energy dispersive X-ray (EDS)

The scanning electron microscopy (SEM) and the energy-dispersive X-ray spectroscopy (EDS) have been developed to observe the morphology and determine the elemental analysis or chemical characterization [50–52].

So, the surface morphology of the copper samples in acidified 3.0 wt % NaCl without and with 200 ppm of extracted CiO after 16 h of immersion was investigated using SEM (Fig. 6) analysis and the chemical composition of the formed products was analyzed using EDS (Fig. 7). It could be seen that copper coupon from the free solution, Fig. 6a display a very rough surface with large rusts and some cracks distributed all through the surface owing to the aggressive attack by the aggressive solution. The scratched was however significantly low in the presence of 200 ppm CiO (Fig. 6b) which demonstrated more even and smoother surface. This smoother surface morphology indicates the formation of a protective CiO film on copper surface [53].

However, the EDS analysis was conducted to investigate the nature of the form of a protective layer. Fig. 7 shows the EDS spectra and the chemical composition of copper surface without and with 200 ppm CiO. The characteristic copper peak intensity (99.51% in wt.) in the uninhibited solution (Fig. 7a) was superior to copper peak intensity (88.38% in wt. of Cu) in inhibiting solution (Fig. 7b), providing a knowledge about the thickness of the protective film formed. However, the EDS data indicated the apparition of O and C peaks, approving the adsorption CiO on the copper surface. This indicates that adsorbed CiO molecules shield copper surface from the corrosive attack by forming a protective film.

The SEM images and EDS analysis were in accordance with the polarization results and the EIS tests. The same concordance were observed by Rami K. Suleiman and al., when they study the corrosion and fouling protection performance of biocide-embedded hybrid organosiloxane coatings on mild steel in a saline medium [54].

3.4. Inhibition efficiency comparison with other green inhibitors

In order to highlight the inhibition efficiency of the extracted CiO, its comparison with other eco-friendly corrosion inhibitors was expected, and the obtained results are presented in Table 4. It is remarked that the inhibition efficiency of the extracted CiO for copper in acidified 3 wt% NaCl solution, was comparatively and even better than many eco-friendly compounds used for corrosion inhibition copper in aggressive media [55–58]. It yet shows good corrosion inhibition performance.

Table 4
Inhibition efficiency comparison of the extracted CiO with other green corrosion inhibitors.

Inhibitors	Systems	Optimum Concentration	Inhibition efficiency	References
Cysteine	Copper / 0.6 M NaCl	16 mM	83.95	[54]
	Copper /1.0 M HCl	20 mM	82.24	
Caffeine	Copper /0.1 M H_2SO_4	10 mM	72.00	[55]
Olive leaf extract	Copper / 0.5 M NaCl	0.48 mM	90	[56]
amino-3-(phenyldiazenyl) benzo [4,5] imidazo[1,2-a] pyrimidin-2(1H)-one	Copper/ 3.5 wt% NaCl	0.8 mM	88.04	[57]
Extracted CiO	Copper/3 wt.%NaCl (at pH = 2)	200 ppm	89.0	This work

Agreeing to the literature, some synthesized products are nowadays difficult to obtain and seem expensive, so there is quiet a great challenge for their varied industrial application [59]. Nevertheless, it concludes that the tested CiO compound has a great application potential in the field of anticorrosion.

3.5. DFT calculations and molecular dynamics simulations

In order to determine and take more information about the essential constituents of CiO responsible for the corrosion inhibition of copper in acidified 3.0 wt% NaCl, DFT calculations and MD simulations for *trans*-cinnamaldehyde (P46), δ-cadinene (P8) and β-cubebene (P5) molecules has been employed using three methods. Gaseous phase optimized structures, and highest occupied and lowest unoccupied molecular orbital (HOMO and LUMO) electron density of the neutral form of the principal constituents of extracted CiO are revealed in Fig. 8. It is remarked for three molecules that they have a planar geometries. This geometry trends to aid maximum interactions between molecules and metal surface, contributing therefore their good anticorrosion efficiencies [60–62]. In addition, the gen of electron density distributions of

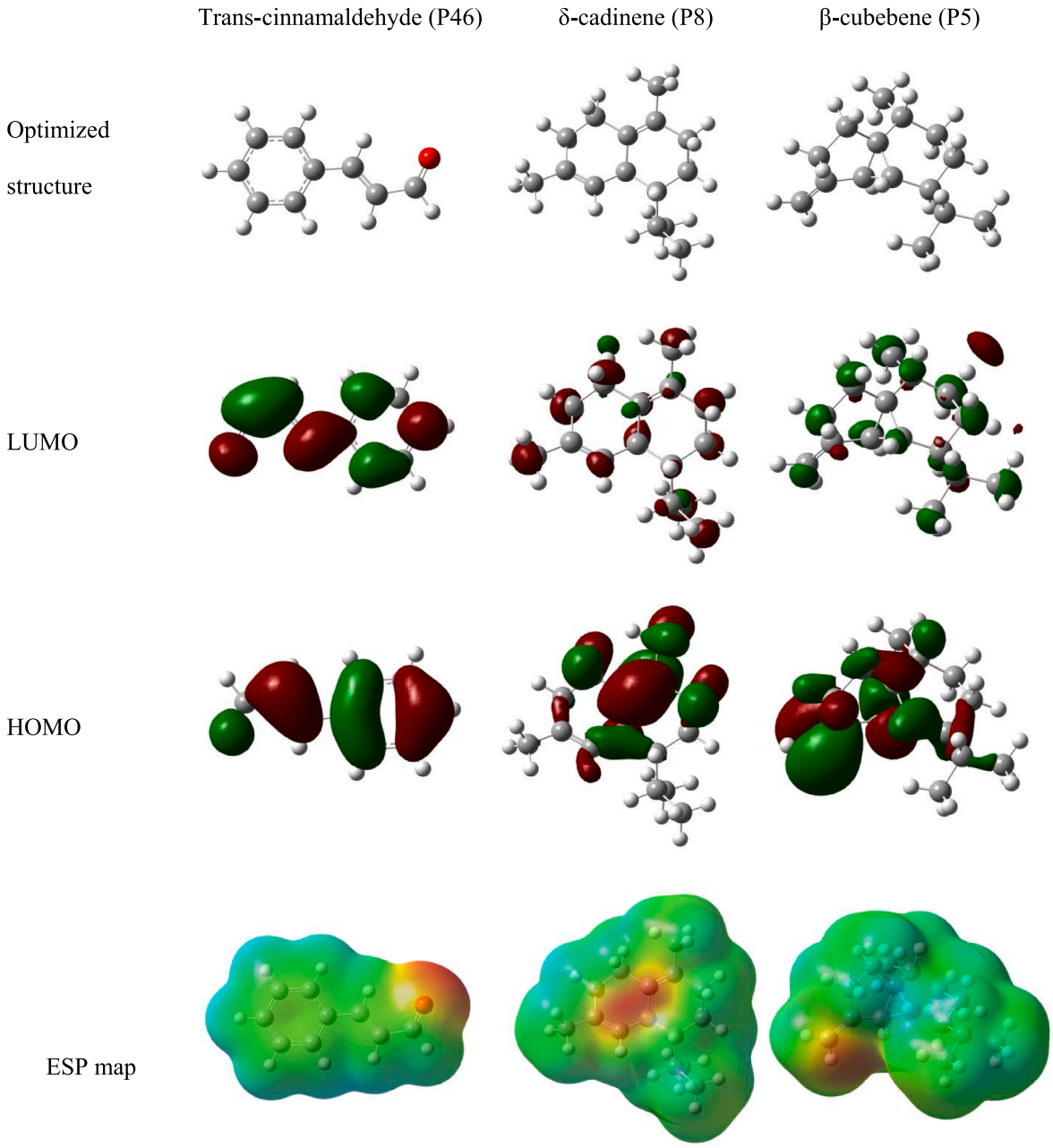

Fig. 8. Optimized structures, HOMOs, LUMOs and ESP maps for three inhibitor molecules.

Table 5
Calculated quantum chemical descriptors for three compounds P46, P8 and P5 using B3LYP method.

Compounds	*trans*-cinnamaldehyde (P46)	δ-cadinene (P8)	β-Cubebene (P5)
E_{HOMO} (eV)	−6.5411	−5.7237	−5.9332
E_{LUMO} (eV)	−2.2675	−0.7821	−0.7663
Δ*E* (eV)	4.2736	4.9416	5.1669
η (eV)	2.1368	2.4708	2.5835
σ (eV^{-1})	0.4680	0.4047	0.3871
χ (eV)	4.4043	3.2529	3.3497
μ (eV^{-1})	−4.4043	−3.2529	−3.3497
ω	4.5391	2.1412	2.1717
ε	0.2203	0.4670	0.4605
ω^{+}	1.7013	0.7111	0.7138
ω^{-}	7.0084	4.0765	4.1695
Δ*N*	0.0973	0.3171	0.2845
α	102.5389	152.5057	149.8279
DM	4.1774	0.3791	0.9740

HOMO offers some suggestions about the electrons donating ability of the molecules to an accepting species with low energy. From Fig. 8, it is noted that the presence of –O atom π-electrons in P46 determine its extent of electron donation and it could readily engage in interaction molecules/metal. For other two compounds P8 and P5, the presence of π-electrons determines their extent of electron donation to metal surface. These findings suggest that the neutral form of these molecules has a good affinity for donating electrons to copper atoms. Thus, the obtained quantum chemical data for the neutral form of P46, P8, and P5 molecules are registered in Table 5. Using these parameters as indices for determining the probable compounds responsible for the obtained inhibition potentials of the tested extract CiO. It is obtained that the order of E_{HOMO} is: P8 (- 5.7237 eV) > P5 (- 5.9332 eV) > P46 (- 6.5411 eV), suggesting that P8 will adsorb more strongly on copper surface than P5 and P46, which is responsible for the obtained inhibition efficiency of extracted CiO. Indeed, the trend of E_{LUMO} is: P5 (-0.7663 eV) > P8 (-0.7821 eV) > P46 (-2.2675 eV), indicating that P46 has the lowest

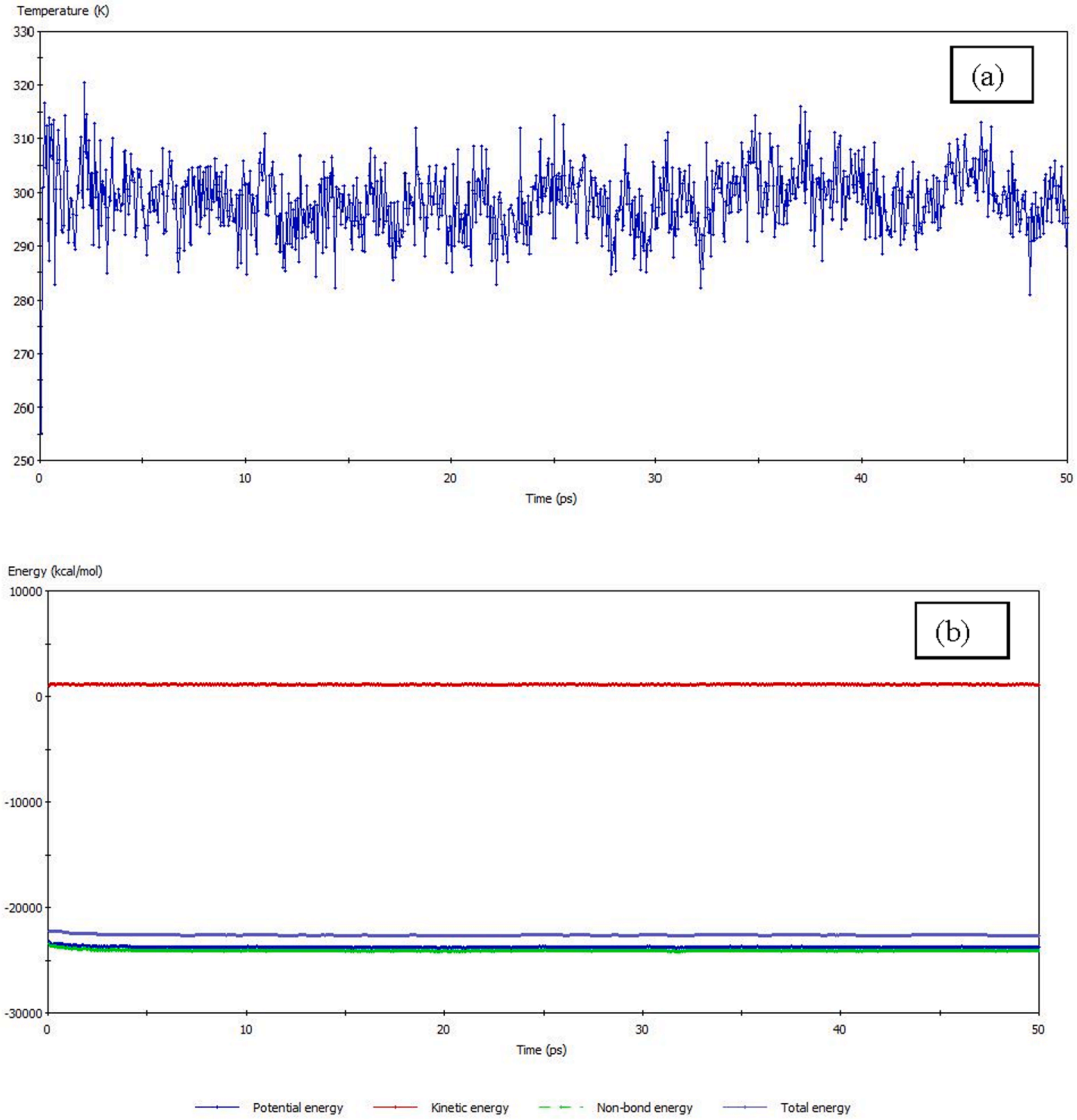

Fig. 9. Trans-cinnamaldehyde (P46) molecule adsorbed on Cu (1 1 1) surface: (a) temperature equilibrium curve and (b) energy fluctuation curve.

energy, suggesting that is ready to accept electrons from copper atomic orbitals. This trend of E_{LUMO}, does not reflect the observed order of E_{HOMO}. Therefore, the order of the energy gap, ΔE is: P46 (4.2736 eV) < P8 (4.9416 eV) < P5 (5.1669 eV), and the same trend was observed for the hardness η (or its reciprocal of softness, **σ**): P46 (2.1368 eV) < P8 (2.4708 eV) < P5 (2.5835 eV). In fact, the lowest values of ΔE and η for P46 involve that it is the most reactive of the three constituents, aiding also its coordination with the copper surface, facilitating its adsorption on copper surface and accordingly raises its anticorrosion efficiency.

Thus, the trend of polarizability α is: P46 (102.5389) < P5 (149.8279) < P8(152.5057), indicating that P8 has the tendency to polarize than P5 and P46. In addition, it is obtained that the electronegativity χ (or μ = - χ) follows the order: P8 (3.2529 eV) < P5 (3.3497 eV) < P46 (4.4043 eV), suggesting that P8 tends to discharge its loosely bound electrons more simply than P46 and P5.

On the other, the order of electrophilicity ω values is: P8 (2.1412 eV) < P5 (2.1717 eV) < P46 (4.5391 eV), indicating that P8 has less electrophilicity value, which has the tendency to accept the electrons and it is effective against corrosion [63,64]. This trend of ω was confirmed by the trend for electron accepting power ω^{+}, which is as follows: P8 (0.7111) < P5 (0.7138) < P46 (1.7013). Furthermore, the trend of electron donating power ω- is : P8 (4.0765) < P5 (4.1695) < P46 (7.0084), indicating that P46 has the tendency to give the electrons to copper atoms and it is effective against corrosion. In the contrast, the trend for nucleophilicity ε, which is as follows: P8 (0.4670) > P5 (0.4605) > P46 (0.2203), indicating that P8 has the greatest tendency to give the electrons to copper atoms.

However, the order of ΔN follows: P8 (0.3171) > P5 (0.2845) > P46 (0.0973), suggesting that P8 has the ability to donate a higher fraction of electrons to the copper atoms than P5 and P46. Indeed, the inverse tendency of the dipole moments, μ, of the tested molecules: P46 (4.1774 D) > P5 (0.9740 D) > P8 (0.3791 D). For this parameter, the researchers are not undisputed about its influence on corrosion inhibition. Some have shown that a rise of μ leads to decrease of the corrosion inhibition efficiency and vice versa, suggesting that lower values of μ will favor the accumulation of molecules on the metallic surface [65,66]. In contrast, some researchers have shown that a rise of μ can lead an increase of the inhibition efficiency and vice versa, which could be related to the dipole–dipole interaction of molecules and metal surface [65–67]. For this, the obtained trend can be indicated that P46 and P8 have the superlative adsorption affinity on copper surface than P5.

Therefore, it is noticed that the majority of the above calculated quantum chemical parameters, indicate that P8 and P46 are the responsible continent for anticorrosion efficiency, with the

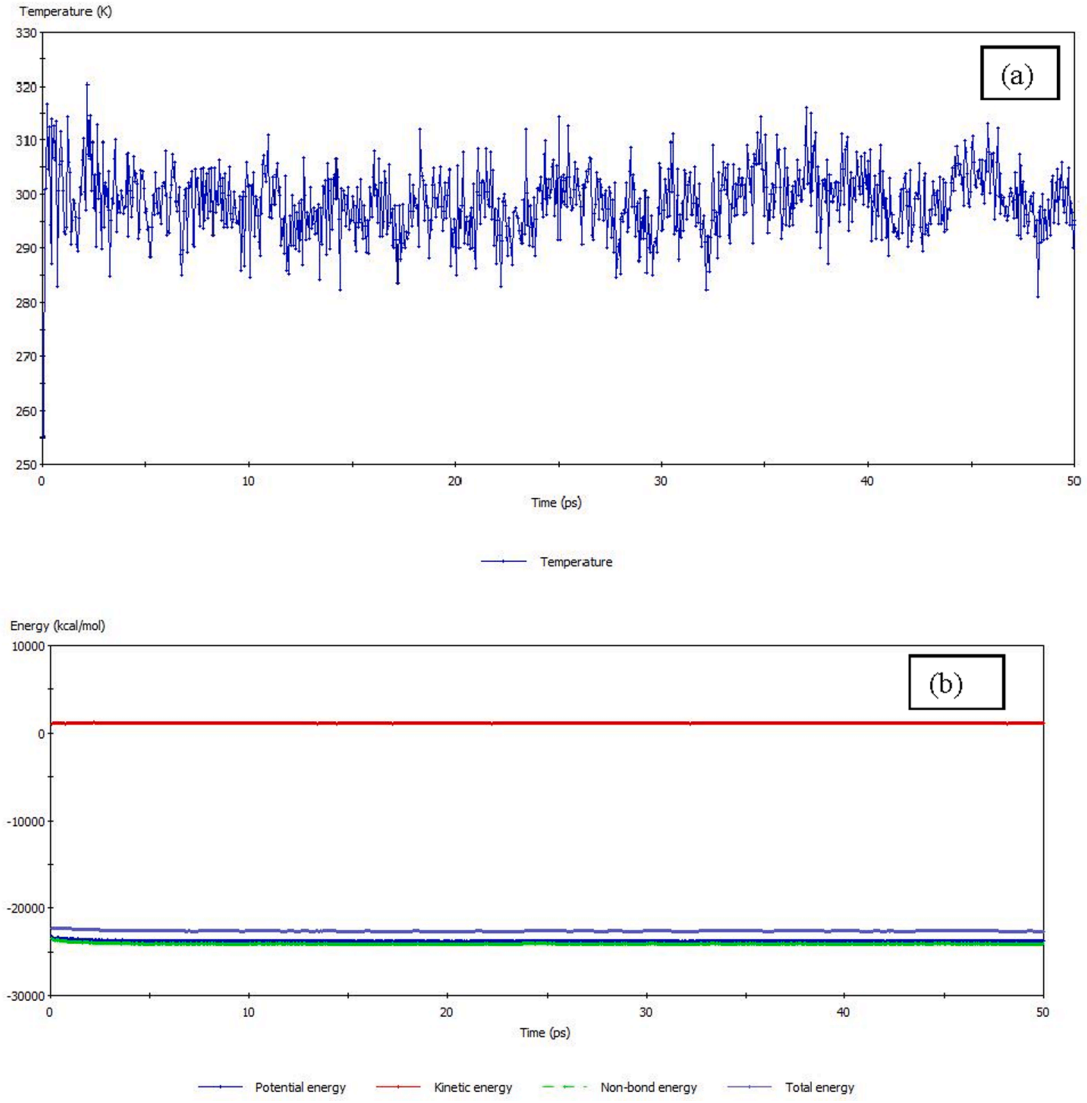

Fig. 10. δ-cadinene (P8) molecule adsorbed on Cu (1 1 1) surface: (a) temperature equilibrium curve and (b) energy fluctuation curve.

predominance of P8. Therefore, it can be concluded that the performance of extracted CiO can be attributed to P8 (δ-cadinene).

The interaction between P46, P8 and P5 compounds and the Cu (1 1 1) and CuO_2(1 1 0) surface in the acidified 3.0 wt% NaCl medium was analyzed by molecular dynamics simulations. It is found that the system touched equilibrium only if both temperature and energy touched balance for three compounds as indicated by Figs. 9, 10 and 11. It is obtained also that the system tended to become equilibrated.

Fig. 12 indicates the possibility of the adsorption of P46, P8 and P5 molecules on copper (1 1 1) and oxide copper (1 1 0). From these figures, it is noted that P8 molecule is parallel to the copper (1 1 1) surface through the benzene ring, contrary to other molecules P46 and P5 and other oxide copper (1 1 0) surface. In addition, it is apparent from the related figure that inhibitor molecules approach to the copper surface via heteroatoms (P8). Consequently, the exposed part of copper surface is minimized by the covering of P8 molecules, stopping corrosive particles, such as proton, water and chloride ions from getting adsorbed on the copper surface. Therefore, the anticorrosion is achieved.

In addition, the calculated adsorption energy values give important signs about corrosion inhibition efficiencies of molecules. The more negative adsorption energy values represent the powerful corrosion inhibition performance. Thus, the adsorption energy (E_{ads}) values for the systems are listed in Table 6. It is found that the trend of the values of E_{ads} follows the order: P5 (-61.071 kJ mol^{-1}) > P46 (-58.070 kJ mol^{-1}) > P8 (-42.938 kJ mol^{-1}) on Cu (1 1 1) and P8 (-21.220 kJ mol^{-1}) > P46 (-20.066 kJ mol^{-1}) > P5 (-19.591 kJ mol^{-1}) on CuO_2 (1 1 0). Therefore, the high absolute value of the E_{ads} shows that strong adsorption of P8 occurs on the oxide copper (1 1 0) surface (corroded surface) [68,69]. As a result, it can be concluded that the performance of extracted CiO can be attributed to P8 (δ-cadinene).

4. Conclusion

In the first stage, the effect of green extracted CiO compound on copper corrosion inhibition in acidified 3.0 wt% NaCl medium has been studied by using electrochemical measurement and SEM/EDAX analysis. In the second stage, the DFT calculations and the molecular dynamics simulation were used to identify the responsible elements of the major constituents of CiO for corrosion inhibition. The following conclusions are:

- Potentiodynamic polarization curves indicated that the extracted CiO decreases the cathodic current density and shifts the corrosion potential more negative, indicating that is cathodic-type inhibitor.
- Electrochemical impedance spectroscopy indicated that the presence of CiO changes the dissolution mechanism of copper and its

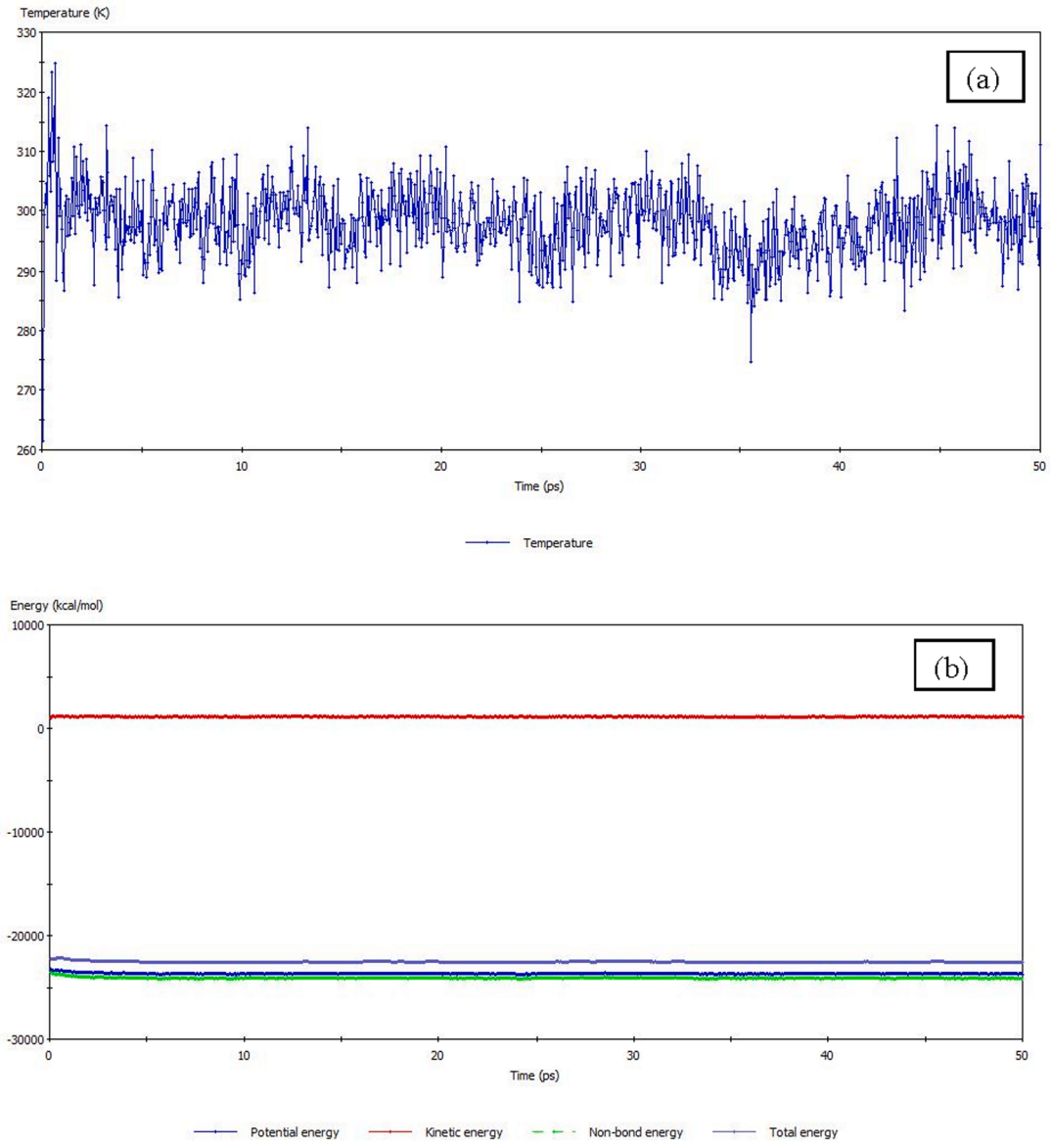

Fig. 11. β-cubebene (P5) molecule adsorbed on Cu (1 1 1) surface: (a) temperature equilibrium curve and (b) energy fluctuation curve.

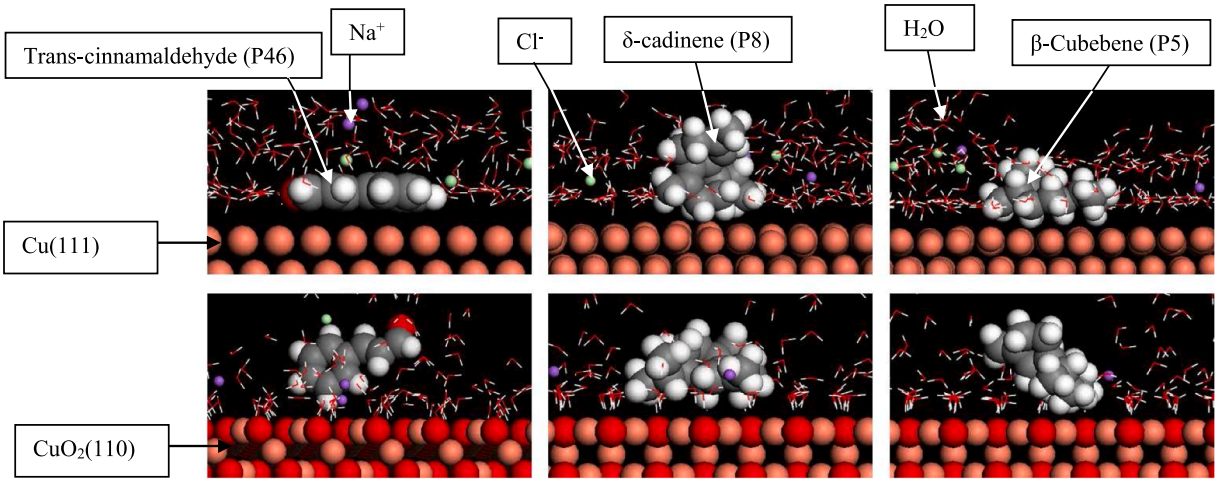

Fig. 12. Configurations of P46, P8 and P5 molecules adsorbed on Cu (1 1 1) and CuO_2 (1 1 0) surface in acidified 3.0 wt% NaCl solution.

Table 6
Calculated adsorption energy values of P46, P8 and P5 on Cu (1 1 1) and Cu_2O (1 1 0) surfaces.

Surfaces	Compounds	E_{total} (kJ mol^{-1})	$E_{surface+H2O}$ (kJ mol^{-1})	$E_{inhibitor}$ (kJ mol^{-1})	$E_{adsorption}$ (kJ mol^{-1})
Cu (1 1 1)	P46	−2393.952	−2318.228	−17.654	−58.070
	P8	−23756.261	−23726.842	13.518	−42.938
	P5	−23716.754	−23759.171	103.489	−61.071
Cu_2O (1 1 0)	P46	−4039.913	−3998.324	−21.522	−20.066
	P8	−4602.810	−4590.611	9.021	−21.220
	P5	−3964.615	−4039.804	94.780	−19.591

inhibition efficiency increases with its concentration to get up a maximum value of 89% at 200 ppm.

- The SEM/EDS analysis in the presence of 200 ppm CiO indicated that copper surface became smooth and exempt for all corrosion products compared to rough and crack surface for free solution, confirming the protection offered by CiO.
- Reasonably good agreement was found between current–potential, electrochemical impedance spectroscopy measurements and SEM/EDS analysis.
- The major calculated quantum chemical parameters obtained from DFT calculations such as E_{HOMO}, E_{LUMO}, ΔE, α, ω, ε, ΔN and μ indicated that the responsible for anticorrosion efficiency is P8 and P46, with the predominance of P8.
- The molecular dynamics simulation showed that the adsorption energy follows the order: P5 (-61.071 kJ mol^{-1}) > P46 (-58.070 kJ mol^{-1}) > P8 (-42.938 kJ mol^{-1}) on Cu (1 1 1) and P8 (-21.220 kJ mol^{-1}) > P46 (-20.066 kJ mol^{-1}) > P5 (-19.591 kJ mol^{-1}) on CuO_2 (1 1 0), indicating a strong adsorption of P8 on oxide copper (1 1 0) surface. It is obtained also that P8 is adsorbed on copper (1 1 1) surface in a closely parallel manner through the benzene ring in contrast of other products P45 and P5 and oxide copper (1 1 0).
- Molecular dynamics simulation confirms DFT calculation results, where the responsible of anticorrosion performance is P8.

Declaration of Competing Interest

The authors declare that they have no known competing financial interests or personal relationships that could have appeared to influence the work reported in this paper.

References

[1] E.M. Sherif, R.M. Erasmus, J.D. Comins, Corrosion of copper in aerated synthetic sea water solutions and its inhibition by 3-amino-1,2,4-triazole, J. Coll. Inter. Sci. 309 (2007) 470–477.
[2] H. Otmacic, J. Telegdi, K. Papp, E. Stupnisek-Lisac, Protective Properties of An Inhibitor Layer Formed on Copper in Neutral Chloride Solution, J. Appl. Electrochem. 34 (2004) 545–550.
[3] E. M. Sherif, S.-M. Park, Inhibition of Copper Corrosion in 3.0% NaCl Solution by N-Phenyl-1,4-phenylenediamine, J. Electrochem. Soc., 152 (2005) 428-433.
[4] H.O. Curkovic, E. Stupnisek-Lisac, H. Takenouti, the influence of pH value on the efficiency of imidazole based corrosion inhibitors of copper, Corros. Sci. 52 (2010) 398–405.
[5] Y.-C. Pan, Y. Wen, X.-Y. Guo, P. Song, S. Shen, Y.-P. Du, 2-Amino-5-(4-pyridinyl)-1,3,4-thiadiazole monolayers on copper surface: Observation of the relationship between its corrosion inhibition and adsorption structure, Corros. Sci. 73 (2013) 274–280.
[6] E. M. Sherif, S. M. Park, 2-Amino-5-ethyl-1,3,4-thiadiazole as a corrosion inhibitor for copper in 3.0% NaCl solutions, Corros. Sci., 48 (2006) 4065-4079.
[7] M. Finsgar, I. Milosev, B. Pihlar, Inhibition of Copper Corrosion Studied by Electrochemical and EQCN Techniques, Acta Chimica Slovenica 54 (2007) 591–597.
[8] M.A. Amin, Weight loss, polarization, electrochemical impedance spectroscopy, SEM and EDX studies of the corrosion inhibition of copper in aerated NaCl solutions, J. Appl. Electrochem. 36 (2006) 215–226.
[9] K.M. Ismail, Electrochemical preparation and kinetic study of poly(*o*-tolidine) in aqueous medium, Electrochimica Acta 52 (2007) 3883–3888.
[10] P. Durainatarajana, M. Prabakaranb, S. Ramesha, V. Periasamy, Surface protection of copper in 3% NaCl solution by using 1-(n-butyl)imidazole self-assembled monolayer, Materials Today: Proceedings 5 (2018) 16226–16236.
[11] C.-C. Li, X.-Y. Guo, S. Shen, P. Song, T. Xu, Y. Wen, H.-F. Yang, Adsorption and corrosion inhibition of phytic acid calcium on the copper surface in 3 wt% NaCl solution, Corros. Sci. 83 (2014) 147–154.
[12] G. Kılınççeker, H. Demir, The inhibition effects of cysteine on the corrosion behaviour of copper in 3.5% NaCl solution, Anti-Corros. Meth. Mater., 60 (2013) 134–142.
[13] S.M. Sherif, Effects of 2-amino-5-(ethylthio)-1,3,4-thiadiazole on copper corrosion as a corrosion inhibitor in 3% NaCl solutions, Appl. Surf. Sci. 252 (2006) 8615–8623.
[14] C.-T. Wang, S.-H. Chen, H.-Y. Ma, C.-S. Qi, Protection of copper corrosion by carbazole and N-vinylcarbazole self-assembled films in NaCl solution, J. Appl. Electrochem. 33 (2003) 179–186.
[15] M. Scendo, M. Hepel, Inhibiting properties of benzimidazole films for Cu(II)/Cu(I) reduction in chloride media studied by RDE and EQCN techniques, J. Electroanal. Chem. 613 (2008) 35–50.
[16] K.F. Khaled, Guanidine derivative as a new corrosion inhibitor for copper in 3% NaCl solution, Mater. Chem. Phys. 112 (2008) 104–111.
[17] A. Tawfik, Saleh, Nanomaterials: Classification, properties, and environmental toxicities, Environmental Technology & Innovation 20 (2020), 101067.
[18] A. Tawfik, Saleh, Trends in the sample preparation and analysis of nanomaterials as environmental contaminants, Trends in Environmental, Analytical Chemistry 28 (2020), e00101.
[19] A. Tawfik, Saleh, Characterization, determination and elimination technologies for sulfur from petroleum: Toward cleaner fuel and a safe environment, Trends in Environmental, Analytical Chemistry 25 (2020), e00080.
[20] A. Tawfik, Saleh, Carbon nanotube-incorporated alumina as a support for MoNi catalysts for the efficient hydrodesulfurization of thiophenes, Chemical Engineering Journal 404 (2021), 126987.
[21] Omar S. BaghabraAl-Amoudi, AbdullahA. Al-Homidy, Mohammed Maslehuddin, Tawfik A. Saleh, Method and Mechanisms of Soil Stabilization Using Electric Arc Furnace Dust, Scientific reports 7, 46676 (2017) DOI: 10.1038/srep46676.
[22] A. Tawfik, Saleh, Mukaila A, Ibrahim, Advances in functionalized Nanoparticles based drilling inhibitors for oil production, Energy Reports 5 (2019) 1293–1304.
[23] Azeem Ranaa, Mohammad K. Arfajb, Tawfik A. Saleh, Advanced developments in shale inhibitors for oil production with low environmental footprints – A review, Fuel 247 (2019) 237–249.
[24] M. Khaled, Ismail, Evaluation of cysteine as environmentally friendly corrosioninhibitor for copper in neutral and acidic chloride solutions, Electrochimica Acta 52 (2007) 7811–7819.
[25] E. Rocca, G. Bertrand, C. Rapin, J.C. Labrune, Inhibition of copper aqueous corrosion by non-toxic linear sodiumheptanoate: mechanism and ECAFM study, J. Electroanal. Chem. 503 (2001) 133–140.
[26] S.A. Abd El-Maksoud, Some phthalazin derivatives as non toxic corrosion inhibitors for copper in sulphuric acid, Electrochimica Acta, 49 (24) (2004) 4205-4212.
[27] F. Sílvio de Souza, C. Giacomelli, R. Simões Gonçalves, A. Spinelli, Adsorption behavior of caffeine as a green corrosion inhibitor for copper, Materials Science and Engineering C, 32 (2012) 2436-2444.
[28] K. Dahmani, M. Galai, M Cherkaoui, A. El hasnaoui, A. El Hessni, Cinnamon essential oil as a novel eco-friendly corrosion inhibitor of copper in 0.5 M Sulfuric Acid medium, J. Mater. Env. Sci. 8 (2017) 1676-1689.
[29] K. Dahmani, M. Galai, A. Elhasnaoui, B. Temmar, A. El Hessni, M. Cherkaoui, Corrosion resistance of electrochemical copper coating realized in the presence of essential oils, Der Pharma Chemica 7 (2015) 566–572.
[30] G. Kılınççeker, M. Baş, F. Zarifi, K. Sayın, Experimental and Computational Investigation for (E)-2-hydroxy-5-(2-benzylidene) Aminobenzoic Acid Schiff Base as a Corrosion Inhibitor for Copper in Acidic Media, Iran J Sci Technol Trans Sci (2020), https://doi.org/10.1007/s40995-020-01015-x.
[31] G. Kılınççeker, S. Çelik, Electrochemical adsorption properties and inhibition of copper corrosion in chloride solutions by ascorbic acid: experimental and theoretical investigation, Ionics 19 (2013) 1655–1662, https://doi.org/10.1007/s11581-013-0902-5.
[32] C. Kun, S. Huyuan, Z. Xia, H. Baorong, Investigation of Novel Gemini Surfactant with Long Chain Alkyl Ammonium Headgroups as Corrosion Inhibitor for Copper in 3.5% NaCl, Int. J. Electrochem. Sci. 9 (2014) 8106–8119.
[33] N. Islam, S. Kaya, (Eds.). (2018). Conceptual Density Functional Theory and Its Application in the Chemical Domain. CRC Press.
[34] T. Tsuneda, J.W. Song, S. Suzuki, K. Hirao, On Koopmans' theorem in density functional theory, J. chem. Phys. 133 (17) (2010), 174101.
[35] R.G. Parr, L.V. Szentpaly, S. Liu, Electrophilicity Index, J. Amer. Chem. Soc. 121 (9) (1999) 1922–1924.
[36] P. K. Chattaraj, S. Giri, S. Duley, Electrophilicity Index, Chem. Rev. 111 (2) (2011) PR43–PR75.
[37] J.L. Gazquez, A. Cedillo, A. Vela, Electrodonating and Electroaccepting Powers, J. Phys. Chem. A 111 (10) (2007) 1966–1970.
[38] D. Kumar, N. Jain, V. Jain, B. Rai, Amino acids as copper corrosion inhibitors: A density functional theory approach, Appl. Surf. Sci. 514 (2020), 145905.
[39] L. Guo, J. Tan, S. Kaya, S. Leng, Q. Li, F. Zhang, Multidimensional insights into the corrosion inhibition of 3,3-dithiodipropionic acid on Q235 steel in H_2SO_4 medium: A combined experimental and *in silico* investigation, J. Coll. Inter. Sci. 570 (2020) 116–124.
[40] B. El Ibrahimi, A. Jmiai, K. El Mouaden, R. Oukhrib, A. Soumoue, S. El Issami, L. Bazzi, "Theoretical evaluation of some α-amino acids for corrosion inhibition of

copper in acidic medium: DFT calculations, Monte Carlo simulations and QSPR studies", Journal of King Saud University – Science, 32(1) (2020) 163-171. DOI 10.1016/j.jksus.2018.04.004.
[41] B. El Ibrahimi, Atomic-scale investigation onto the inhibition process of three 1,5-benzodiazepin-2-one derivatives against iron corrosion in acidic environment, Colloid and Interface Science Communications 37 (2020), 100279, https://doi.org/10.1016/j.colcom.2020.100279.
[42] R. Oukhrib, B. El Ibrahimi, H. Abou Oualid, Y. Abdellaoui, S. El Issami, L. Bazzi, M. Hilali, H. Bourzi, "In silico investigations of alginate biopolymer on the Fe (110), Cu (111), Al (111) and Sn (001) surfaces in acidic media: Quantum chemical and molecular mechanic calculations", Journal of molecular liquids, 312 (2020) 113479. DOI 10.1016/j.molliq.2020.113479.
[43] H. Bourzi, R. Oukhrib, B. El Ibrahimi, H. Abou Oualid, Y. Abdellaoui, B. Balkard, S. El Issami, M. Hilali, L. Bazzi, C. Len, "Furfural Analogs as Sustainable Corrosion Inhibitors – Predictive Efficiency using DFT and Monte Carlo Simulations on the Cu (111), Fe(110), Al(111) and Sn(111) Surfaces in Acid Media", Sustainability, 12(8) (2020) 3304.
[44] B. El Ibrahimi, L. Bazzi, S. El Issami, The role of pH on the corrosion inhibition of tin using proline amino acid: Theoretical and experimental investigations, RSC Advances 10 (2020) 29696–29704, https://doi.org/10.1039/D0RA04333H.
[45] M.M. Antonijevic, S.C. Alagic, M.B. Petrovic, M.B. Radovanovic, A.T. Stamenkovic, The Influence of pH on Electrochemical Behavior of Copper in Presence of Chloride Ions, Int. J. Electrochem. Sci. 4 (2009) 516–524.
[46] H. Otmačić, E. Stupnišek-Lisac, Copper corrosion inhibitors in near neutral media, Electrochim. Acta 48 (8) (2003) 985–991.
[47] E.M. Sherif, Su-Moon Park, 2-Amino-5-ethyl-1,3,4-thiadiazole as a corrosion inhibitor for copper in 3.0 % NaCl solutions, Corros. Sci., 48(12)(2003) 4065-4079.
[48] E.M. Sherif, Effects of 2-amino-5-(ethylthio)-1,3,4-thiadiazole on copper corrosion as a corrosion inhibitor in 3% NaCl solutions, Appl. Surf. Sci. 252 (24) (2006) 8615–8623.
[49] E. M. M. Sutter, F. Ammeloot, M. J. Pouet, C. Fiaud, R. Couffignal, Heterocyclic compounds used as corrosioninhibitors] correlation between 13C and 1H NMR spectroscopy and inhibitione.ciency, Corros. Sci., 41 (1999) 105-115.
[50] T.A. Saleh, Trends in the sample preparation and analysis of nano-materials as environmental contaminants, Trends in Environmental Analytical Chemistry 28 (2020), e00101.
[51] S. O. Adio, M. H. Omar, M. Asif, T. A. Saleh, Arsenic and selenium removal from water using biosynthesized nanoscale zero-valent iron: A factorial design analysis, Process Safety and Environmental Protection 1 0 7 (2 0 1 7) 518–527.
[52] T. A. Saleh, M. Tuzen, A. Sarı, Polyamide magnetic palygorskite for the simultaneous removal of Hg(II) and methyl mercury; with factorial design analysis, Journal of Environmental Management 211 (2018) 323e333.
[53] K. Haruna, T.A. Saleh, I.B. Obot, S.A. Umoren, Cyclodextrin-based functionalized graphene oxide as an effective corrosion inhibitor for carbon steel in acidic environment, Progress in Organic Coatings 128 (2019) 157–167.
[54] R. K. Suleiman, T. A. Saleh, O. C. S. Al Hamouz, M. B. Ibrahim, A. A. Sorour, B. El Ali, Corrosion and fouling protection performance of biocide-embedded hybrid organosiloxane coatings on mild steel in a saline medium, Surf. Coat. Tech., 324 (2017) 526-535.
[55] M. Khaled, Ismail, Evaluation of cysteine as environmentally friendly corrosion inhibitor for copper in neutral and acidic chloride solutions, Electrochimica Acta 52 (2007) 7811–7819.
[56] F. Sílvio de Souza , C. Giacomelli , R. Simões Gonçalves, A. Spinelli, Adsorption behavior of caffeine as a green corrosion inhibitor for copper, Materials Science and Engineering C, 32 (2012) 2436- 2444.
[57] C. Rahal, M. Masmoudi, R. Abdelhedi, R. Sabot, M. Jeannin, M. Bouaziz, P. Refait, Olive leaf extract as natural corrosion inhibitor for pure copper in 0.5 M NaCl solution: A study by voltammetry around OCP, Journal of Electroanalytical Chemistry 769 (2016) 53–61.
[58] S. Pareeka, D. Jaina, S. Hussain, A. Biswas, R. Shrivastava, Saroj K. Parida, Hemanta K. Kisan, H. Lgazf, Ill-Min Chung, D. Behera, A new insight into corrosion inhibition mechanism of copper in aerated 3.5 wt.% NaCl solution by eco-friendly Imidazopyrimidine Dye: experimentaland theoretical approach. Chemical Engineering Journal 358 (2019) 725–742.
[59] S.M. Tawfik, Ionic liquids based gemini cationic surfactants as corrosion inhibitors for carbon steel in hydrochloric acid solution, J. Mol. Liq. 216 (2016) 624–635, https://doi.org/10.1016/j.molliq.2016.01.066.
[60] C. Verma, M.A. Quraishi, L.O. Olasunkanmi, E.E. Ebenso, L-Proline-promoted synthesis of 2-amino-4-arylquinoline-3-carbonitriles as sustainable corrosion inhibitors for mild steel in 1 M HCl: experimental and computational studies, RSC Adv. 5 (2015) 85417–85430.
[61] N. Errahmany, M. Rbaa, A. S. Abousalem, A. Tazouti, M. Galai, H. El Kafssaoui, M. Ebn Touhami, B. Lakhrissi, R. Touir, Experimental, DFT calculations and MC simulations concept of novel quinazolinone derivatives as corrosion inhibitor for mild steel in 1.0 M HCl medium, J. Molec. Liq., 312(15) (2020) 113413.
[62] M. El Faydy, R. Touir, M. Ebn Touhami, A. Zarrouk, C. Jama, B. Lakhrissi, L. O. Olasunkanmi, E. E. Ebenso, F. Bentiss, Corrosion inhibition performance of newly synthesized 5-alkoxymethyl-8-hydroxyquinoline derivatives for carbon steel in 1 M HCl solution: experimental, DFT and Monte Carlo simulation studies, Phys. Chem. Chem. Phys., 20 (2018) 20167-201187.
[63] A. Tazouti, M. Galai, R. Touir, M. Ebn Touhami, A. Zarrouk, Y. Ramli, M. Saraçoğlu, S. Kaya, F. Kandemirli, C. Kaya, Experimental and theoretical studies for mild steel corrosion inhibition in 1.0 M HCl by three new quinoxalinone derivatives, J. Molec. Liq., 221 (2016) 815–832.
[64] N.O. Obi-Egbedi, I.B. Obot, Inhibitive properties, thermodynamic and quantum chemical studies of alloxazine on mild steel corrosion in H_2SO_4, Corros. Sci. 53 (2011) 263–275.
[65] M. Mahdavian, S. Ashhari, Corrosion inhibition performance of 2-mercaptobenzimidazole and 2-mercaptobenzoxazole compounds for protection of mild steel in hydrochloric acid solution, Electrochim. Acta 55 (5) (2010) 1720–1724.
[66] F. Bentiss, B. Mernari, M. Traisnel, H. Vezin, M. Lagrenee, On the relationship between corrosion inhibiting effect and molecular structure of 2,5-bis(*n*-pyridyl)-1,3,4-thiadiazole derivatives in acidic media: Ac impedance and DFT studies, Corros. Sci. 53 (2011) 487–495.
[67] M. Lagrenée, B. Mernari, N. Chaibi, M. Traisnel, H. Vezin, F. Bentiss, Investigation of the inhibitive effect of substituted oxadiazoles on the corrosion of mild steel in HCl medium, Corros. Sci. 43 (2001) 951–962.
[68] L. Guo, S. Zhu, S. Zhang, Experimental and theoretical studies of benzalkonium chloride as an inhibitor for carbon steel corrosion in sulfuric acid, J. Ind. Eng. Chem. 24 (2015) 174–180.
[69] Y. Qiang, S. Zhang, S. Xu, W. Li, Experimental and theoretical studies of benzalkonium chloride as an inhibitor for carbon steel corrosion in sulfuric acid, J. Coll. Inter. Sci. 472 (2016) 52–59.

Prof. **Rachid Touir** was born in 1977 in Kenitra City, Morocco. He received his Ph.D. in Physics Chemistry, from Ibn Tofail University, Morocco, 2009. He had published more than ***110 papers (92*** indexed in scopus***)*** in international journals. His work has been cited ***2025 total citations*** by ***1123 documents*** with ***h-index*** = ***25*** (since **2006** in **SCOPUS**) and presented several ***communications*** in symposia and national/international meetings. He was honored with the award for the best thesis researcher in Ibn Tofail University since the year 2009. He has developed **3 patents** and he has participated in **6 national research** projects. He has supervised **45 Doctoral** Theses and **80 Master** theses in science and didactics. He is a reviewer at several national and international journals. He is the author of a **3 books**.

His main research interests are in the field of Physical Chemistry, Especially electrochemistry (Corrosion and its inhibition in several media for metals and alloys using various techniques). He is also interested for electroless plating of Ni-P, Ni-Cu-P, Cu-P, Ni-Pd-Cu… and their components in several corrosive medium. He is currently interested in using some quantum chemical methods like density functional theory (DFT) and other semi-empirical methods to study corrosion inhibition efficiencies of organic compounds. He is also interested in the Didactics of physics and chemistry.

Filters Clear All

- *Web of Science* Coverage
- Open Access
- Category
- Country / Region
- Language
- Frequency
- Journal Citation Reports

Refine Your Search Results

INORGANIC CHEMISTRY COMMUNICATIONS Search

Sort By: Relevancy

Search Results

Found 1,802 results (Page 1) Share These Results

Exact Match Found

INORGANIC CHEMISTRY COMMUNICATIONS

Publisher: **ELSEVIER , RADARWEG 29, AMSTERDAM, NETHERLANDS, 1043 NX**

ISSN / eISSN: **1387-7003 / 1879-0259**

Web of Science Core Collection: **Science Citation Index Expanded**

Additional *Web of Science* Indexes: **Current Contents Physical, Chemical & Earth Sciences | Essential Science Indicators**

Share This Journal View profile page

Other Possible Matches

ADVANCES IN INORGANIC CHEMISTRY

Publisher: **ELSEVIER ACADEMIC PRESS INC , 525 B STREET, SUITE 1900, SAN DIEGO, USA, CA, 92101-4495**

ISSN / eISSN: **0898-8838 / 1557-8917**

Web of Science Core Collection: **Science Citation Index Expanded**

Additional *Web of Science* Indexes: **Essential Science Indicators**

Share This Journal View profile page

CHINESE JOURNAL OF INORGANIC CHEMISTRY

Publisher: **CHINESE CHEMICAL SOC , C/O DEPT INT AFFAIRS, SECRETARY OF CHEM SOC, PO BOX 2709, BEIJING, PEOPLES R CHINA, 100080**

ISSN / eISSN: **1001-4861**

Results: 1

(from Web of Science Core Collection)

You searched for: TITLE: (Quantum chemical and molecular dynamic simulation studies for the identification of the extracted cinnamon essential oil constituent responsible for copper corrosion inhibition in acidified 3.0 wt% NaCl medium) ...More

Create an alert

Refine Results

Search within results for...

Publication Years

- 2021 (1)

Refine

Web of Science Categories

- CHEMISTRY INORGANIC NUCLEAR (1)

Refine

Document Types

- ARTICLE (1)

Refine

Organizations-Enhanced

- CUMHURIYET UNIVERSITY (1)
- IBN TOFAIL UNIVERSITY OF KENITRA (1)
- IBN ZOHR UNIVERSITY OF AGADIR (1)
- REG CTR EDUC TRAINING PROFESS CRMEF (1)

more options / values...

Refine

Funding Agencies

Authors

Source Titles

View all options

For advanced refine options, use

Analyze Results

Sort by: Date Times Cited Usage Count Relevance More

1 of 1

Select Page Export... Add to Marked List

Analyze Results

Create Citation Report

1. **Quantum chemical and molecular dynamic simulation studies for the identification of the extracted cinnamon essential oil constituent responsible for copper corrosion inhibition in acidified 3.0 wt% NaCl medium**

By: Dahmani, K.; Galai, M.; Ouakki, M.; et al.

INORGANIC CHEMISTRY COMMUNICATIONS Vo

FEB 2021

View Abstract

Times Cited: 4
(from Web of Science Core Collection)

Usage Count

Select Page Export... Add to Marked List

Sort by: Date Times Cited Usage Count Relevance

Show: 10 per page

1 records matched your query of the 78,725,508 in the data limits you s

INORGANIC CHEMISTRY COMMUNICATIONS

Impact Factor

2.495	1.887
2020	*5 year*

JCR® Category	*Rank in Category*	*Quartile in Category*
CHEMISTRY, INORGANIC & NUCLEAR	21 of 45	Q2

Data from the 2020 edition of Journal Citation Reports

Publisher
ELSEVIER, RADARWEG 29, 1043 NX AMSTERDAM, NETHERLANDS

ISSN: 1387-7003
eISSN: 1879-0259

Research Domain
Chemistry

Close Window